2-28-2023

Unpacking the proteome and metaproteome of the black soldier fly larvae: Efficacy and complementarity of multiple protein extraction protocols

Utpal Bose
Edith Cowan University

Angela Juhasz
Edith Cowan University

Sally Stockwell

Sophia Escobar-Correas
Edith Cowan University

Anna Marcora

See next page for additional authors

10.1021/acsomega.2c04462
Bose, U., Juhasz, A., Stockwell, S., Escobar-Correas, S., Marcora, A., Paull, C., ... & Wijffels, G. (2023). Unpacking the proteome and metaproteome of the black soldier fly larvae: Efficacy and complementarity of multiple protein extraction protocols. ACS Omega, 8(8), 7319-7330. https://doi.org/10.1021/acsomega.2c04462

ACS OMEGA

http://pubs.acs.org/journal/acsodf

Article

Unpacking the Proteome and Metaproteome of the Black Soldier Fly Larvae: Efficacy and Complementarity of Multiple Protein Extraction Protocols

Utpal Bose,* Angela Juhasz, Sally Stockwell, Sophia Escobar-Correas, Anna Marcora, Cate Paull, James A. Broadbent,* and Gene Wijffels

Cite This: *ACS Omega* 2023, 8, 7319−7330

Read Online

ACCESS | Metrics & More | Article Recommendations | Supporting Information

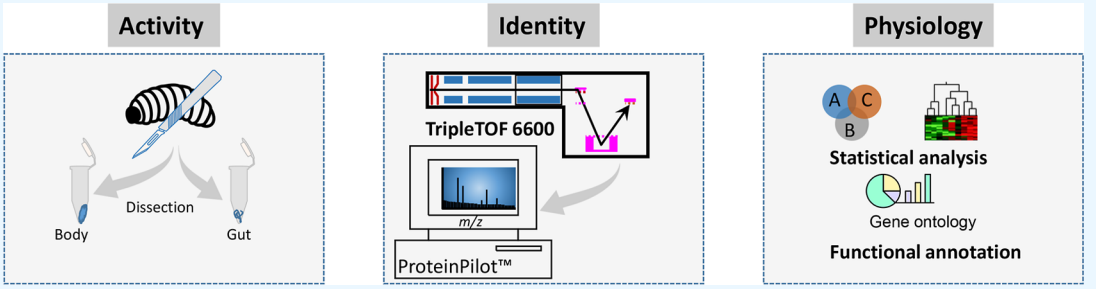

ABSTRACT: The larvae of the black soldier fly (BSF), *Hermetia illucens* (Diptera: Stratiomyidae), have demonstrated the ability to efficiently bioconvert organic waste into a sustainable source of food and feed, but fundamental biology remains to be discovered to exploit their full biodegradative potential. Herein, LC−MS/MS was used to assess the efficiency of eight differing extraction protocols to build foundational knowledge regarding the proteome landscape of both the BSF larvae body and gut. Each protocol yielded complementary information to improve BSF proteome coverage. Protocol 8 (liquid nitrogen, defatting, and urea/thiourea/chaps) was better than all other protocols for the protein extraction from larvae gut samples, and the exclusion of defatting steps yielded the highest number of proteins for the larval body samples. Protocol-specific functional annotation using protein level information has shown that the selection of extraction buffer can affect protein detection and their associated functional classes within the measured BSF larval gut proteome. A targeted LC-MRM-MS experiment was performed on the selected enzyme subclasses to assess the influence of protocol composition using peptide abundance measurements. Metaproteome analysis of the BSF larvae gut has uncovered the prevalence of two bacterial phyla: actinobacteria and proteobacteria. We envisage that using complementary extraction protocols and investigating the proteome from the BSF body and gut separately will expand the fundamental knowledge of the BSF proteome and thereby provide translational opportunities for future research to enhance their efficiency for waste degradation and contribution to the circular economy.

INTRODUCTION

The black soldier fly (BSF), *Hermetia illucens* (Diptera: Stratiomyidae), is recognized for its capacity to efficiently and effectively convert organic waste into a sustainable source of protein for animal feed.[1] The bioconversion process within BSF also produces by-products, such as fat for bioenergy[2] and compost, for use as fertilizer.[3] Additionally, BSF protein derivatives contain bioactive peptides[4] that could effectively protect animals from oxidative damage when used as ingredients in pet food and aquaculture feed formulations.[5] The BSF larvae's potential in recycling waste materials marks them as candidates in future circular economies and nutrient cycling, which have marked opportunities to shift agriculture to more sustainable systems. Yet, the phenotypic selection of insect species for mass-rearing amenable to optimization and suitable to specific environmental criteria such as diet at a commercial scale is not fully understood. Further studies are required to understand the fundamental biochemical pathways that control their growth, fitness, and capability to convert waste into feed.

BSF is not regarded as a pest species and can be easily reared indoors under controlled conditions.[6] The recently sequenced genome of BSF provides an inventory of proteins that may be produced in this species,[7] but the phenotypic proteome that describes the proteins of the larval stages in the context of their

Received: July 15, 2022
Accepted: February 7, 2023
Published: February 20, 2023

environment and diet is currently unknown. Knowledge of the BSF larval proteome can be crucial to understanding the physiological processes in the insects, providing insights into mechanisms of adaptation to altering conditions and traits for selection.

Previous studies of the BSF larval proteome have generated extracts for analysis using various combinations of mechanical disruption of whole larvae, different buffers, and optional defatting. BSF larvae have been mechanically disrupted with a mortar and pestle,[8] liquid nitrogen grinder,[9] or high-throughput crusher[10] to prepare a homogeneous BSF material prior to moving onto protein extraction using a single buffer composition. Previous studies have reported the use of a hexane-based defatting step to remove the lipid prior to extracting the proteins with a urea-based lysis buffer followed by acetone precipitation[9] and the sequential extraction (defatting followed by protein precipitation) of lipids and proteins from BSF larvae.[11] Proteins have also been extracted directly with Tris−HCl lysis buffer containing urea,[10] and urea plus thiourea and Tris−HCl from BSF larvae.[8] Extraction buffers comprised of Tris−HCl and SDS have also been used to extract proteins from several insect species, including BSF larvae.[11,12] Proteins have been extracted either from the whole BSF larvae[8,9] or from the midgut following dissection.[10] Though several proteomics studies were performed using the BSF whole or the dissected larval body, no study has reported on the proteome of the BSF gut.

Protein extraction using a single buffer may limit proteome coverage due to protein solubility preferences, while the analysis of whole insects will dilute the signal from low-abundance proteins beyond detection. Indeed, the BSF larval midgut is known to contain commensal bacterial species,[13] which require careful consideration to achieve detection by mass spectrometry. Six bacterial genera, including *Dysgonomonas*, *Morganella*, *Enterococcus*, *Pseudomonas*, *Actinomyces*, and *Providencia*, were found to be predominantly present in the BSF gut.[13] Additionally, metagenomics studies have shown the influence of diet on the diversity of the BSF gut microbiome;[13−15] however, the BSF gut proteome and metaproteome composition remains underexplored.

Host−microbe interactions are important to perform beneficial roles including stress response, host fitness, and digestion of food.[16] The diversity and changes of gut microbial diversity is poorly understood in BSF larvae, and in particular, the presence of enzymes such as hydrolases within these bacterial communities is unknown. The present study aimed to determine an optimized extraction protocol to deliver a nonbiased, generalized overview of the BSF larval proteome. Comparative analyses were performed on the detected proteins to establish the optimum protein extraction buffer composition for BSF larval body and gut. Additionally, comprehensive functional annotations were performed on the protein- and peptide-level data generated from the larval body and gut. These analyses will guide future investigations of proteome-wide changes in BSF larvae as their potential in waste recycling is delineated and optimized for diverse waste streams.

MATERIALS AND METHODS

Rearing of BSF Larvae. The BSF colony was established from eggs collected from a suburban compost bin in Brisbane, Queensland, Australia, in November 2020. The BSF culture is maintained at the CSIRO Insect Laboratory (Ecosciences Precinct, Dutton Park, Brisbane, Australia) in a constant environment room set at a 14:10 h light−dark cycle, with a 60% relative humidity at 26 °C. At egg hatch, BSF neonates were reared on a mix of 50% Barastoc golden yolk poultry pellets (Melbourne, VIC, Australia) and wheat bran that was mixed with deionized distilled water. Four-day old larvae were then transferred to rectangular glass dishes and fed a diet of commercially sourced mixed vegetables and milk powder.

Approach. The experiment was designed to compare the efficacy of two different mechanical disruption methods (bead beating vs immersion in liquid nitrogen followed by pulverization), the impact of a defatting step, and the use of two different denaturants, the anionic surfactant sodium dodecyl sulfate (SDS) vs chaotropic agents, urea and thiourea, combined with the zwitter-ionic surfactant CHAPS (UTC) in a Tris−HCl-based extraction buffer. The various protocols were abbreviated P1 to P8, where P1 denotes the sequential combination of bead-beating, defatting (DF), and extraction by the Tris buffer containing SDS (i.e., bead beating + DF + SDS); P2, bead-beating + no defatting (NDF) + SDS; P3, signifies the combination of bead-beating, defatting (DF), and the use of the Tris buffer containing UTC (i.e., bead beating + DF + UTC); P4, bead-beating + NDF + UTC; P5 denotes the combination of immersion in liquid nitrogen followed by pulverization, defatting (DF), and the Tris buffer containing SDS (i.e., liquid nitrogen + DF + SDS); P6, liquid nitrogen + NDF + SDS; P7, liquid nitrogen + DF + UTC; and, P8, liquid nitrogen + NDF + UTC. The workflow is presented in Figure 1.

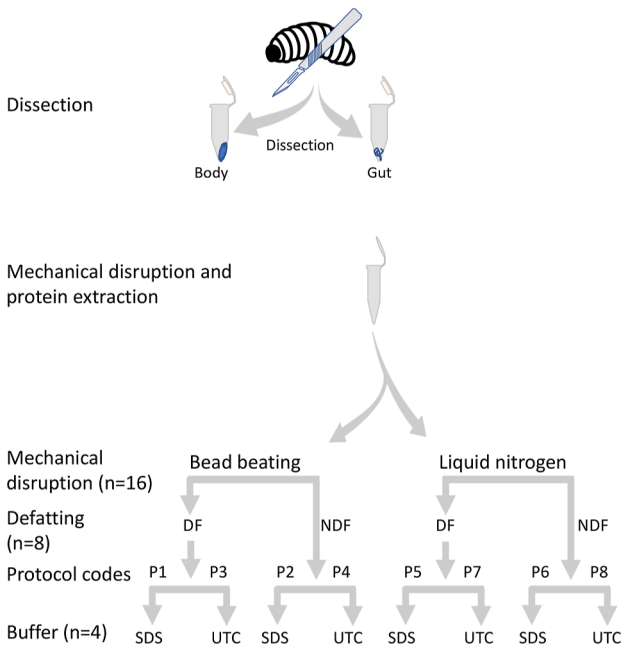

Figure 1. Schematic representing the dissection of BSF larvae and the processing of larval bodies and guts using eight different protocols (P1−P8) in preparation for proteome analyses. Sixteen tissue samples were individually mechanically disrupted by bead beating, and sixteen tissue samples were individually disrupted by snap freezing using liquid nitrogen followed by pulverization. After mechanical disruption, eight individual samples were defatted (DF) or eight individual samples were not (NDF). Finally, protein extraction was performed with buffers containing SDS or urea/thiourea/CHAPS (UTC). Therefore, every protocol is represented by four individual samples.

https://doi.org/10.1021/acsomega.2c04462
ACS Omega 2023, 8, 7319−7330

Dissection of BSF Larvae to Collect the Body and Gut and Tissue Processing. We used four larvae as replicates for each treatment group to capture the biological variances in the samples. In the present study, one larva was treated as a biological replicate, with four biological replicates per group. The body and gut of individual larva were separated and frozen at −80 °C prior to mechanical disruption by either pulverization into a fine powder after immersion in liquid nitrogen or by bead beating. Thirty two twelve day old BSF larvae were individually removed from the diet and rinsed in distilled water (room temperature, RT). The larvae had developed from a single egg lay period of 12 or less hours and were selected for use by experienced entomological staff. The fifth instar larvae, which are characterized by their distinct change in color (tanning) and reduced consumption of diet, were not used for this analysis. Excess water was removed from the larva by blotting on paper a towel. The washed larva was transferred to 20 mL of PBS in a chilled glass Petri dish resting on wet ice. The head and tail of each larva were excised, and an incision was made from head to tail to carefully remove the gut, ensuring the remainder of the body was intact. Each gut and body were immediately placed in separate, pre-weighed tubes sitting on dry ice. The mean wet weights (±SEM) of the larval bodies and the excised guts were 151.5 ± 6.2 and 46.1 ± 3.0 mg. The detailed dissection and sample preparation for the BSF larvae and body samples are given in Supporting Information File S1.

Protein Estimation and Digestion. The Bradford protein assay was used to estimate the protein concentration of the extracts. The detailed assay parameters and steps were recently published by our group.[17,18]

The extracts were subjected to filter-assisted sample preparation (FASP), wherein the protein extract (100 μg) in 200 μL of urea buffer (8 M urea in 0.1 M Tris−HCl, pH 8.0) was loaded to a 30 kDa molecular weight cut-off (MWCO) filter (Millipore, Australia) and centrifuged (16,500×*g*, 15 min). The detailed FASP protocols for protein clean-up and digestion steps were published for insect proteins from our group.[17,18] The resultant dried peptides from filters were resuspended in 50 μL of 0.1% formic acid, and 2 μL (equiv to 4 μg of total protein) was analyzed by LC−MS/MS.

Proteome Measurement, Database Preparation, and Protein Identification. Detailed chromatographic profiles and MS conditions were previously described.[17−19] In brief, 2 μL of peptides were chromatographically separated and detected with an Ekspert nanoLC415 (Eksigent, Dublin, CA) coupled to a TripleTOF 6600 MS (SCIEX, Redwood City, CA). An in-house BSF proteome database was built by combining protein sequences from UniProt-Diptera (accessed on 07-04-2020) translated open reading frame (ORF) sequences derived from two available BSF genome assemblies (Genbank assembly accessions: GCA_001014895.1 and GCA_009835165.1, coded as G1 and G2, respectively) downloaded from NCBI.[18] These protein sequences were merged with the common repository of adventitious proteins (cRAP) sequences and the iRT pseudo-protein sequences (in total, 523,909 sequences). Protein sequences from the Enterobacteriaceae and Actinobacteria phyla were downloaded from UniProtKB and added to the BSF database. This combined BSF and microbial database was used to search BSF gut proteome samples (ProteinPilot automatically generates and concatenates a reversed database for false discovery rate estimation).

ProteinPilot v5.0.3 software (SCIEX), incorporating the Paragon and ProGroup algorithms, was used for peptide and protein identification, respectively. ProteinPilot search parameters were described in detail previously.[17,20] For clarity, peptide-spectrum matches (PSMs) for each BSF larvae file were determined by the Paragon search algorithm,[21] wherein each PSM was allocated an unused score. In addition, the confidence in each identification is calculated as per.[21] Datafiles were searched against the database individually, and then individual replicate files were mapped against the master set of accessions to unify the protein accession numbers. These lists of accession numbers were compiled for each protocol using the SCIEX Protein Alignment template. The protocol lists describing the proteome repertoire were subjected to the downstream comparative and functional analyses.

LC−MS/MRM Method. To assess the performance of extraction protocols, proteins were selected and imported into the Skyline software to identify MRM transitions. Unscheduled methods were exported from Skyline software to refine the MRM methods by using a pooled sample. MRM data were acquired from a pooled sample (injected three times to evaluate reproducibility). The obtained results were used to refine the transitions and schedule retention times. The peptides were selected based on their peak intensity and fully tryptic in nature, with no variable modifications or missed cleavages. Detailed MRM optimization parameters were previously reported by our research team.[20]

Statistical Analysis and Data Visualization. Principal component analysis (PCA) and hierarchical clustering analysis (HCA) were performed using SIMCA software (v 17.0, Sartorius). The data matrix consisting of the unused protein score for PCA was $\log_{10}$ transformed and pareto scaled, while *Z*-score scaling was used for HCA. UpSet plots and Venn diagrams were generated using the Intervene Shiny app.[22] Functional annotations for the protocol-specific proteins were conducted using the BLAST2GO module within OmicsBox software, and Unipept v 4.0 was used for metaproteome analysis using peptide level information.[23] Annotated proteins were mapped to enzyme codes, and the mapped enzymes, including their codes and annotations, were used to report the overrepresentation of enzymes. GraphPad Prism software v 9.0 and Microsoft Excel were used for functional annotation and data visualization. A Student's *t*-test and an ordinary one-way ANOVA were used to compare the protein yields and protein and peptide identification numbers obtained from the eight sample preparation protocols (P1−P8).

RESULTS

The efficacy of a suite of protein extraction protocols using alternative tissue disruption methods, defatting (or not), and detergent selection was assessed at multiple levels. The larval body with gut removed, and the isolated gut were extracted using the suite of protocols (Figure 1). Assessment of efficacy included simple quantitative measures of protein and peptide yields through enumeration of protein identifications and representation by functional annotation. Finally, the extracts generated by the suite of extraction protocols were assessed for the relative abundance of enzymes involved in detoxification pathways by liquid chromatography-multiple reaction monitoring-mass spectrometry (LC-MRM-MS). In the case of the gut tissue, the ability to detect signatures of the microbiota and its diversity was also attempted.

https://doi.org/10.1021/acsomega.2c04462
ACS Omega 2023, 8, 7319−7330

Table 1. Yields of Protein (μg) and Enumeration of Proteins and Peptides Detected Following Eight Extraction Protocols (P1−P8) From the Body of the Black Soldier Fly (*Hermetia illucens*)[a]

buffer ± DF	DF-SDS			NDF-SDS			DF-UTC			NDF-UTC		
protocol	P1			P2			P3			P4		
mechanical disruption	protein yield	proteins	peptides	protein yield	proteins	peptides	protein yield	Proteins	peptides	protein yield	proteins	peptides
bead beating (replicates)	143.2	1051	4202	70.0	953	4140	65.2	831	3459	95.3	1217	4466
	109.3	686	2964	113.1	910	3601	74.5	873	3895	106.0	943	4118
	70.6	849	3597	90.4	910	3745	90.0	847	3825	84.7	893	4076
	82.3	954	4096	107.3	750	3404	74.8	850	3777	102.3	905	3920
mean	101.3	885.0	3714.8	95.2	880.8	3722.5	76.1	850.3	3739.0	97.1	989.5	4145.0
sd	32.2	156.2	565.8	19.5	89.5	311.5	10.3	17.3	192.9	9.4	153.2	230.3
		P5			P6			P7			P8	
liquid nitrogen + pulverization (replicates)	39.6	16*	35*	78.9	1041	4408	33.6	624	2685	80.1	924	3794
	27.9	1002	4340	74.6	1020	4386	36.9	777	3123	46.8	994	4199
	40.7	874	4169	104.9	1088	4431	36.3	822	3108	62.8	908	3950
	34.0	833	3716	87.3	44*	120*	34.4	788	3168	71.1	994	4143
mean	35.6	903.0	4075	86.4	1049.7	4408.3	35.3	752.8	3021	65.2	955.0	4021.5
Sd	5.9	88.2	322.4	13.4	34.5	22.5	1.4	87.9	225.4	14.1	45.5	185.4

[a]Four biological replicates (individual larva) were allocated to each extraction protocol. The number of proteins identified at global 1% FDR (and distinct peptides identified with local 95% confidence) are shown. DF, defatted; NDF, nondefatted; SDS, SDS based extraction buffer; UTC, urea, thiourea, CHAPS extraction buffer, P, protocol. Protein yield is given as μg protein/mg wet tissue (body) weight. *Replicates were removed from the downstream annotation and analysis.

Table 2. Yields of Protein (μg) and Enumeration of the Proteins and Peptides Detected Following Eight Extraction Protocols (P1−P8) From the Gut of the Black Soldier Fly (*Hermetia illucens*).[a]

buffer ± DF	DF-SDS			NDF-SDS			DF-UTC			NDF-UTC		
protocol	P1			P2			P3			P4		
mechanical disruption	protein yield	proteins	peptides	protein yield	proteins	peptides	protein yield	proteins	peptides	protein yield	proteins	peptides
bead beating (replicates)	27.31	558	1023	32.83	744	2095	41.17	803	2265	9.09	323	677
	59.48	499	991	53.94	404	1732	37.75	840	2704	28.46	574	1427
	46.27	417	822	16.90	766	2120	121.95	872	2519	12.87	519	1160
	33.19	533	1070	24.77	682	1887	51.08	919	2363	11.97	458	1120
mean	41.6	501.8	976.5	32.1	649.0	1958.5	63.0	858.5	2462.8	15.6	468.5	1096.0
SD	14.3	61.5	108.0	15.9	167.2	183.6	39.7	49.2	191.9	8.7	108.0	310.8
		P5			P6			P7			P8	
liquid nitrogen + pulverization (replicates)	27.36*	1075*	2833*	33.45	694	1428	25.42	851	2388	40.01	1179	3316
	8.80	482	1119	27.11	744	1642	26.43	634	2035	35.95	1031	3071
	8.16	462	1136	35.50	733	1508	32.59	683	1851	45.76	891	2822
	2.93	365	809	24.62	729	1635	10.63			28.24		
mean	6.6	436.3	1021.3	30.2	725.0	1553.3	32.1	722.7	2091.3	37.5	1033.7	3069.7
SD	3.2	62.6	184.1	5.1	21.6	103.8	15.9	113.8	272.9	7.4	144.0	247.0

[a]Four biological replicates (individual larva) were allocated to each extraction protocol. The number of proteins identified at global 1% FDR (and distinct peptides identified with local 95% confidence) are shown. P, protocol. Protein yield is given as μg protein/mg wet gut weight. *Replicates were removed from the downstream annotation and analysis.

Assessment of Protein Yield and Protein and Peptide Enumeration from the Larval Body and Gut. Bead beating as a mechanical disruption method yielded 66% more total protein from the larval body than liquid nitrogen snap freezing and exhibited much less variation between replicates ($P < 0.0001$; mean ± SD, bead beating: 92.4 ± 20.6 μg protein/mg wet body weight vs liquid nitrogen: 55.6 ± 24.1 μg protein/mg wet body weight) (Table 1). There were no significant effects of the mechanical disruption method, the DF step, or the choice of buffer on protein yield from the gut tissue. P4 and P5 returned the least protein (Table 2) and were or tended to be significantly lower in yield than all other protocols. The comparison of protocol-dependent protein yields for body and gut samples is given in Supporting Information File S2.

LC-MS-based discovery proteomics data acquisition followed by database searching was performed at the level of the individual replicate extracts to detect and quantify the number of proteins (1% FDR), peptides (95% confidence), and spectral mapping information from the BSF larval body extracts (Tables 1; S1). One replicate each from of P5 and P6 was excluded from the analysis due to the failure of data acquisition by the mass spectrometer. The mechanical disruption method did not influence the number of protein identifications ($P = 0.913$; mean protein identifications ± SD, bead beating: 901.4 ± 119.1 vs liquid nitrogen: 906 ± 128.0).

https://doi.org/10.1021/acsomega.2c04462
ACS Omega 2023, 8, 7319−7330

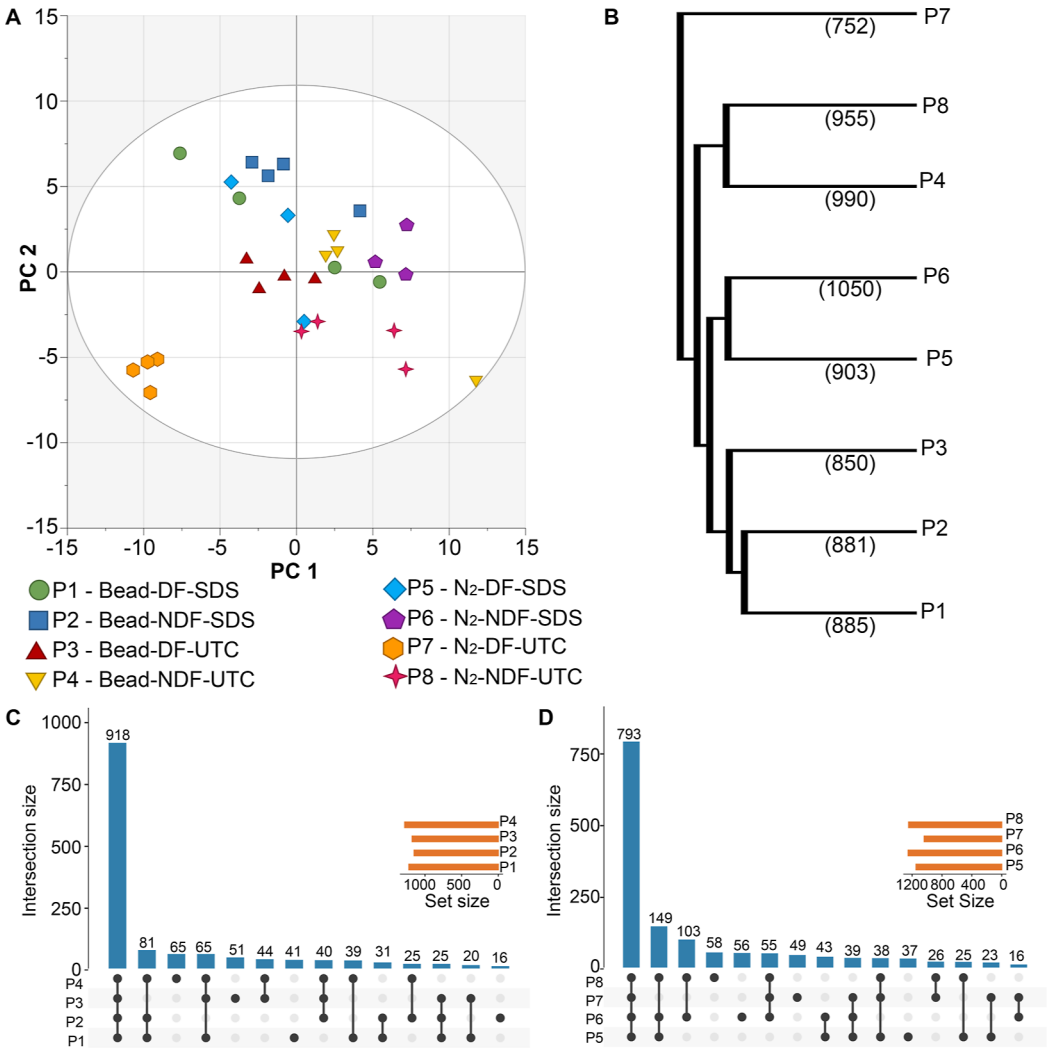

Figure 2. Summary of protein enumeration and repertoire from the BSF larval body extracted with eight different protocols. (A) Principal component analysis scores plotted based on unused protein scores and colored by extraction protocol. (B) Hierarchical clustering analysis (HCA) based on the sum of the unused protein scores of the replicates from each protocol. Numbers in the brackets are the mean number of proteins detected from each protocol. UpSet plots showing the distribution of shared and unique protein identifications resulting from bead beating (C) or liquid nitrogen (D) mechanical disruption protocols. Protein accessions generated from the protein alignment tool were used to prepare figures (C, D).

The DF step resulted in ∼14% fewer protein identifications (P = 0.0048; mean protein identifications ±SD, DF: 844.1 ± 108.1 vs NDF: 963.3 ± 105.5). There was no effect of buffer choice on the number of protein identifications (P = 0.429). The comparative analysis between protocols for the body in terms of protein, peptide, and spectral mapping is given in Supporting Information File S2. Likewise, we also performed protein and peptide level comparisons for the larval gut samples (Supporting Information File S2). In terms of protein and peptide identification, P8 was found to be superior to other tested protocols for the larval gut samples.

Comparative Analyses of the Proteome Repertoire Detected in the BSF Larval Body Using Different Protocols. The LC−MS data sets were searched against the custom-made BSF database, and the protein identifications aligned to the protein accessions across all samples. Thereafter, the aligned unused protein scores generated from ProteinPilot software for each extract were used to compare the quality of the protein identifications for that extract and its relationship to all other extracts using PCA. The resulting score plot shows the extraction protocol-dependent clustering. An initial assessment of the PCA scores plot resulted in removing a single replicate from P5 and P6 as those observations were deemed outliers based on Hotelling's T2 (95% confidence). The three-component PCA model captured 23.5% of the total variance, where PC1 and PC2 components explained 11.6 and 6.2%, respectively (Figure 2A), indicating a moderate uniformity of the protein identification quality across the extracts. The P7 replicates formed a distinct cluster in the lower PC1/PC2 quadrant, indicating the high reproducibility of this protocol. Using the sum of the unused protein scores for each extraction protocol, the HCA analysis showed clear relationships between the protocols (Figure 2B).

To understand the protein repertoires underlying the differing clusters, a master list of protein accessions (1574 proteins) built by removing redundancies and unifying the protein accessions, was loaded into the SCIEX Protein Alignment template. The extraction-specific protein identification sets were compared against the master set to assess differences in the respective proteomes (Figure 2C). The

https://doi.org/10.1021/acsomega.2c04462
ACS Omega 2023, 8, 7319−7330

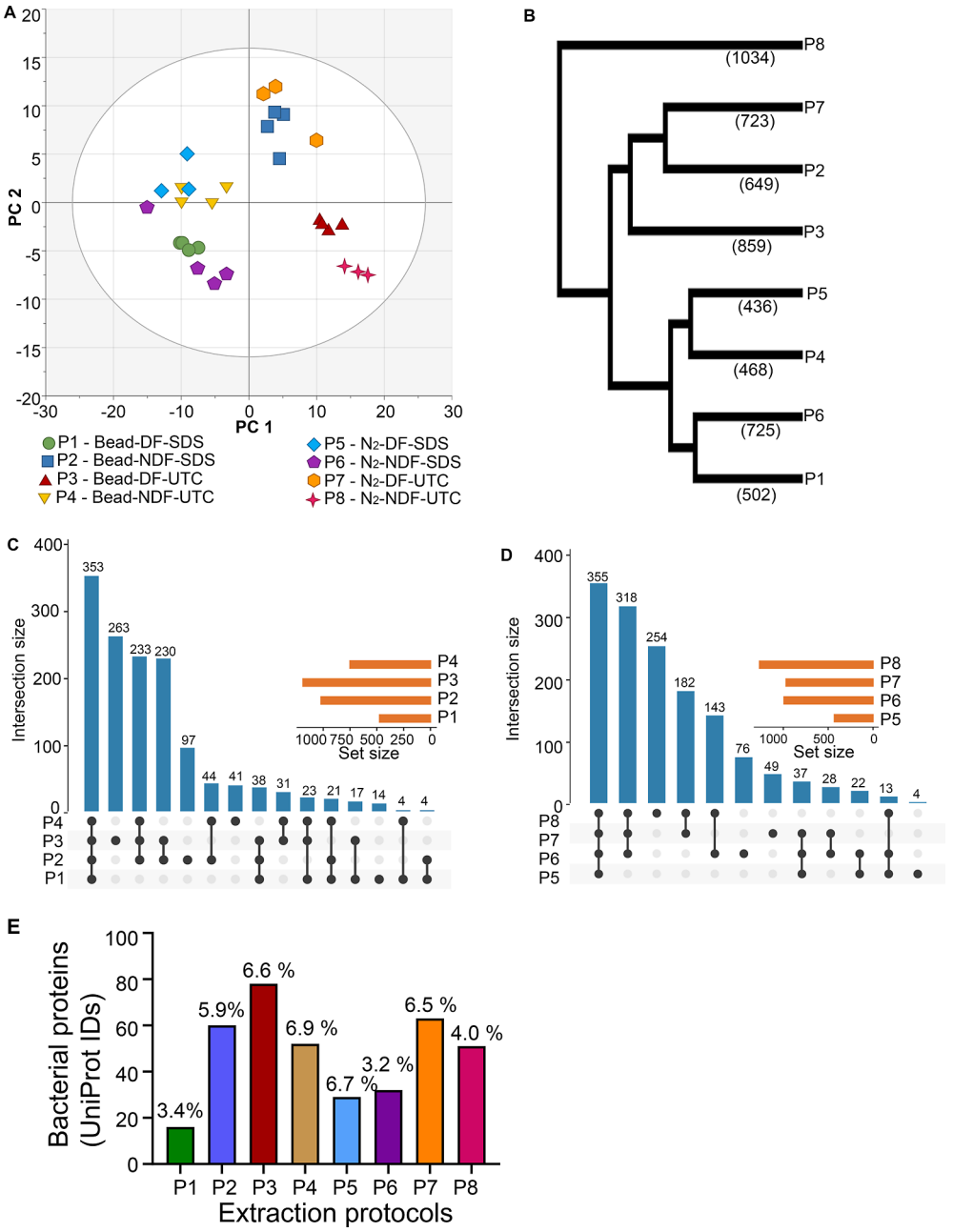

Figure 3. Summary of protein enumeration and repertoire from BSF larval gut extracted with eight different protocols. (A) Principal component analysis based on the unused protein scores of identified proteins. (B) Hierarchical clustering analysis (HCA) based on the mean of the unused protein scores of the replicates from each protocol. Numbers in the brackets are the mean number of proteins detected from each protocol. The UpSet plots show the distribution of shared and unique proteins identified in the different extracts of larval gut generated by bead beating (C) or liquid nitrogen (D) disruption protocols. Protein accessions generated from the protein alignment tool were used to prepare figures (C,D). (E) Histogram reports the number of unique bacterial protein identifications detected in the extracts of each protocol; the % bacterial proteins of total protein identifications for each protocol are indicated.

number of protein accessions across the eight extraction protocols was similar, ranging from 1039−1277, with a mean (±SD) of 1189 (±78) protein accessions. The bead beating protocols (P1−P4) coextracted 918 proteins, or 58.3% of the 1574 proteins in the master protein set. Each protocol extracted a small number of unique proteins, that is, 41, 16, 51, and 65, unique to P1−P4, respectively (Figure 2C). The extracts produced by liquid nitrogen coextracted 793 proteins (50.4% of the total NR protein set) across the P5−P8 extracts. Due to the lower protein and peptide yield of the P7 extracts, the common set of proteins in the liquid nitrogen protocols was smaller than that obtained from the bead beating protocols. The DF extracts produced by P5 and P7 contained 37 and 49 unique proteins, respectively, whereas the NDF extracts produced by P6 and P8 collectively contributed a total of 103 unique proteins to the master set (6.5%, Figure 2D). As P7 yielded the lowest protein identifications (1034), there was a greater distribution of shared proteins among the remaining extract groups (Figure 2D).

Comparative Analyses of the Proteome Repertoire Detected BSF Larval Gut Using the Different Protocols. A comparative analysis was performed on the Unused Protein

https://doi.org/10.1021/acsomega.2c04462
ACS Omega 2023, 8, 7319−7330

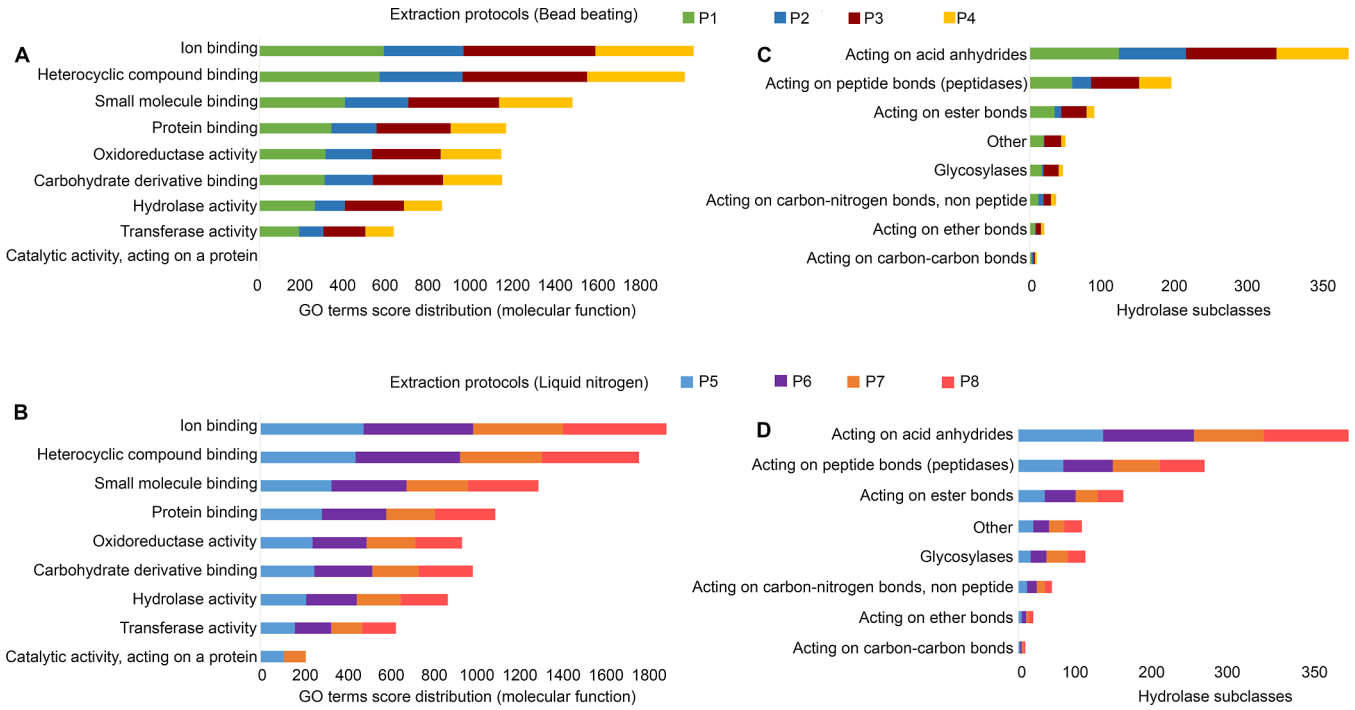

Figure 4. Functional annotation of proteins detected in extracts of the BSF larval body generated by the eight extraction protocols (P1−P8). Representative level 3 GO terms (molecular functions) obtained from the proteins detected in the larval body mechanically disrupted (A) with bead beating (P1−P4) or (B) in liquid nitrogen pulverization (P5−P8). Major enzyme subclasses with hydrolase activity were detected from each extraction protocol either preceded by bead beating (C) or in liquid nitrogen (D). The *x*-axis represents the number of protein sequences (assignments) mapped to individual hydrolase activity subclasses.

Scores number of proteins identified from the BSF larval gut. The PCA plot shows the clustering based on the Unused Protein Scores when emphasizing the maximum variance in the data set (P1−P8, Figure 3A). The extracts produced by P3 and P8 were clustered tightly and located in the lower right quadrant, well separated from the extracts of the other protocols, which were dispersed through the remaining quadrants. P1, P4, P5, and P6 replicates were separated in PC1 from P2, P3, P7, and P8. In the PCA analysis, PC1 explained 30% of the variance within the data set, while PC2 captured 11.5% of the variance. It should be noted that P3 and P8 gut extracts contained the highest yield of protein identifications (Table 2). The HCA plot shows the clustering of extraction protocols based on the protocol average Unused Protein Scores (i.e., the average of the Unused Protein Scores of the replicates of each protocol, Figure 3B). In this analysis, P8 is distinct from all other protocols, but otherwise, the clustering is similar to that seen in the PCA plot (Figure 3B), with the replicates of P1, P4, P5, and P6 clustering together and a second cluster formed by the replicates of P2, P3, and P7.

The shared protein set among the bead beating protocols was 353 proteins, equating to 22% of the total protein identifications. The largest number of unique proteins, 263 proteins, were provided by the P3 extracts (16.5% the total identifications), and 230 proteins were coextracted by the P2 and P3 protocols (Figure 3C). The liquid nitrogen mechanical disruption protocols (P5−P8) led to a complex distribution of shared and unique proteins (Figure 3D). The common protein set for the P5−P8 numbered 355 proteins, which was 22.2% of the total identifications, while P6−P8 shared 318 proteins (19.9% of the total). Of the liquid nitrogen protocols, the P8 extracts had the highest unique protein yield (254; 15.9% of the total). The combination of liquid nitrogen disruption with UTC buffer contributed a further 182 unique proteins (Figure 3D). The extracts produced by P1 and P5, protocols that combined the DF step with extraction in the SDS buffer, possessed the lowest protein identifications (i.e., 430−470 protein accessions). The protocol-specific raw data were searched against the bacterial protein databases to investigate the presence of bacterial proteins (Figure 3E). The histogram indicates that of the bead beating protocols, the P3 extracts contained the highest number of bacterial proteins, that is, 78 proteins, representing 6.6% of the P3 identifications. Overall, a positive effect of DF on the yield of bacterial proteins was discerned among the liquid nitrogen protocols (Supporting Information File S2).

Functional Annotation of Protein Sets Derived from BSF Larval Body Extracts. Functional annotation was conducted using level 3 GO terms on the proteins detected in the BSF body extracts (Figure 4A,B). The assignments were dominated by the GO terms ion binding and heterocyclic compound binding, which accounted for 19.5 and 18.7% of the total number of assignments across all extraction protocols, respectively. The terms, small molecule binding, protein binding, carbohydrate derivative binding, and oxidoreductase activity each catered for 10−14% of the total assignments. The enzyme related terms, hydrolase activity, transferase activity, and catalytic activity, acting on a protein, covered the remaining assignments. The overall distribution of level 3 GO assignments among the extracts was similar (Figure 4A,B).

Interest in the enzymic capacity of BSF to degrade various feedstocks and waste streams prompted a closer examination of the hydrolase activity term, which was allocated 8.5% of assignments. Eight hydrolase activity subclasses were assigned to the larval body proteome, with the two most dominant

https://doi.org/10.1021/acsomega.2c04462
ACS Omega 2023, 8, 7319−7330

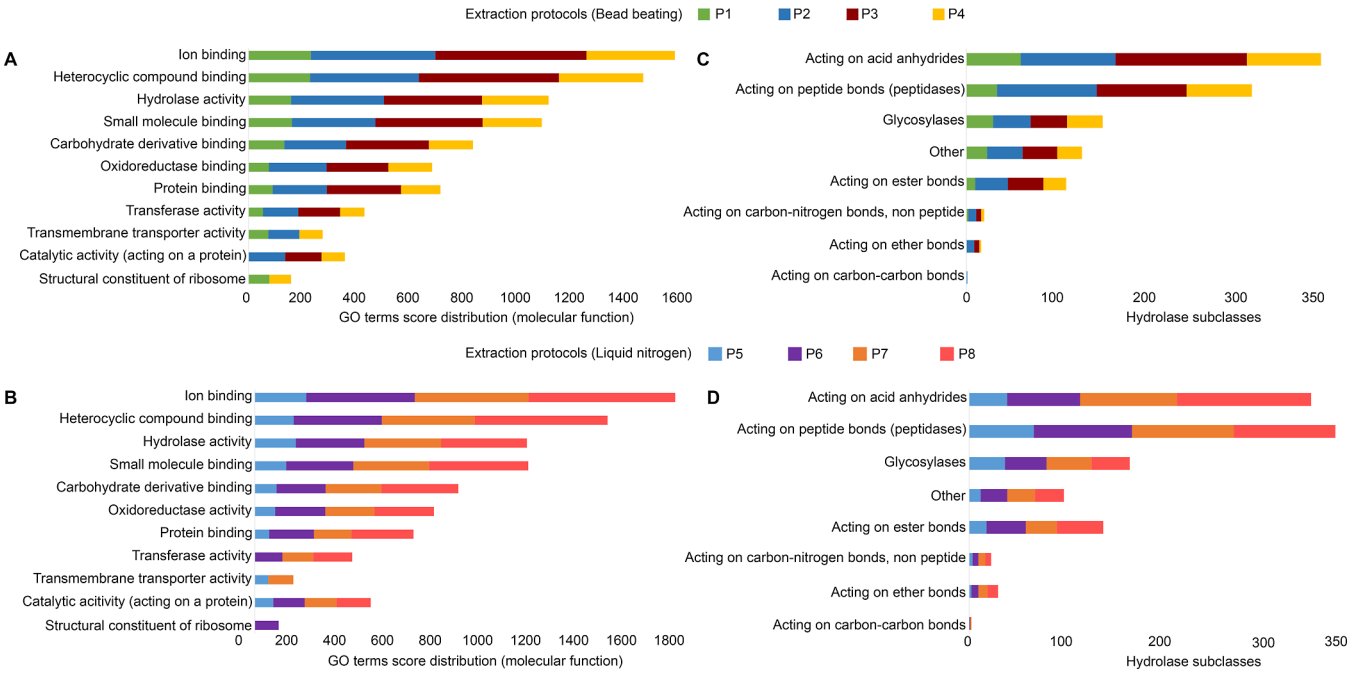

Figure 5. Functional annotation of proteins detected in extracts of BSF larval gut generated by the eight extraction protocols (P1−P8). Assignment of level 3 GO terms (molecular function) for larval gut proteins mechanically disrupted by (A) bead beating (P1−P4) or (B) liquid nitrogen (P5−P8). The major hydrolase activity subclasses were identified from larval gut extracts mechanically disrupted by bead beating (C) and liquid nitrogen (D).

terms being those acting on acid anhydrides and those acting on peptide bonds with 45 and 23% of the total hydrolase activity assignments, respectively (Figure 3C,D; Supporting Information File S2). There was no effect of DF on assignments to the hydrolase activity subclasses; however, the SDS buffer was enriched for assignments to act on carbon−nitrogen bonds.

Functional Annotation of the Protein Identifications Derived from the BSF Larval Gut. Gene ontology (GO) analysis was performed on the identified proteins in the gut extracts generated from each protocol (Figure 5A,B). Of the 11 third level GO terms assigned across the extracts of all protocols, the foremost were ion binding activity and heterocyclic compound binding with ∼17−19% of the total assignments across all protocols, followed by small molecule binding and hydrolase activity with 13% each. Across the protocols, the distribution of assignments to the level 3 GO terms was similar.

There were no significant effects of DF or buffer on level 3 GO term assignment to the gut extracts. Inspection of the enzyme subclass assignments within hydrolase activity revealed almost equal allocations to acting on acid anhydrides and acting on peptide bonds, with 32 and 30%, respectively, of the total number of assignments across all protocols (Figure 5C,D; Supporting Information File S2). Other terms allocated assignments were glycosylases (14%) and acting on ester bonds (11%). Other classes received ∼10% of total assignments; this subclass refers to hydrolases that do not fall within the specific subclasses. Despite the apparent numerical differences between protocols (Figure 5C,D), there were no significant effects of mechanical disruption, DF or buffer choice on the allocation of assignments to hydrolase subclasses. When looking at % assignment of total assignment to hydrolase activity, there was a tendency for the overrepresentation of acting on peptide bonds in the liquid nitrogen disrupted extracts (bead beating vs liquid nitrogen: mean ± SD, 27.0 ± 4.3% vs 32.6 ± 3.9%, P = 0.102), while the bead beaten extracts were allocated higher % assignment to other classes (11.7 ± 1.9% vs 8.1 ± 1.1%, P = 0.016).

Effect of Protocol on Apparent Abundances of Targeted Enzymes Quantified by LC-MRM-MS in the BSF Larval Body and Gut Extracts. Relative quantification of nine proteins in the body extracts and seven proteins in the gut extracts generated by the eight extraction protocols was performed by liquid chromatography-multiple reaction monitoring-mass spectrometry (LC-MRM-MS). A method was developed to determine the relative abundances of enzymes representing four different families: the carboxylic esterases (CEs), P450s, simple lipases, and phenol oxidases (PO). The heatmap visualization shows the relative abundance of the targeted enzymes in the gut and body across the protocols (Figure 6). Detection of the two P450 proteins in body tissue was significantly affected by the mechanical disruption method;

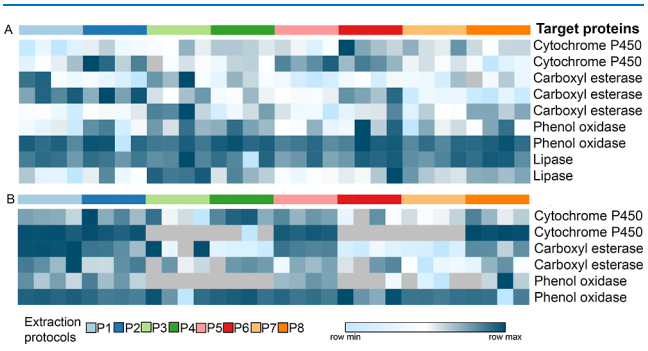

Figure 6. LC-MRM-MS-based quantitation for selected proteins from the BSF larvae body (A) and gut (B) samples extracted with eight extraction protocols.

https://doi.org/10.1021/acsomega.2c04462
ACS Omega 2023, 8, 7319−7330

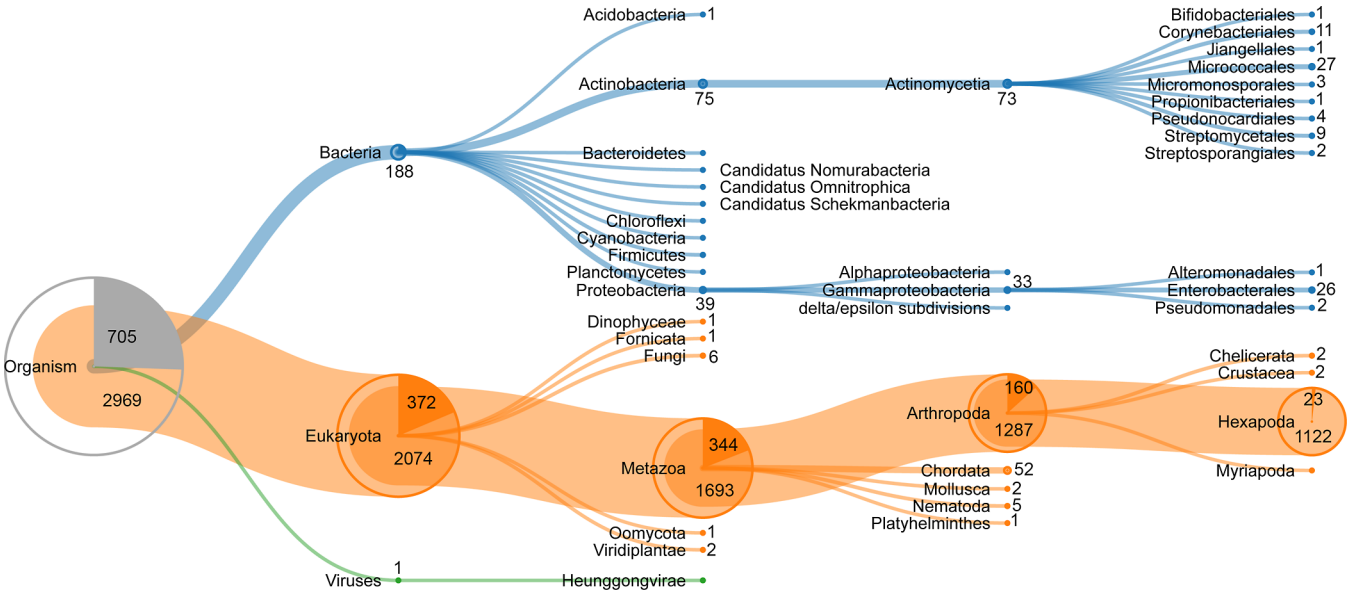

Figure 7. Metaproteome analysis of the BSF larval gut proteome. The Treeview map shows the taxonomic-level mapping of peptides detected in the BSF larval gut.

liquid nitrogen snap freezing increased the apparent abundance of the P450s by ~39% (P = 0.045) and there was a significant increase in relative abundance when UTC was used as the extraction buffer (~42%, P = 0.035). Interestingly, bead beating tended to be the better disruption method for the gut P450s, with a 60% increase in relative abundance (P = 0.062), and there was a tendency toward an effect of DF. NDF gut extracts displayed 54% higher relative abundance (P = 0.082).

Apparent abundances of the CEs in the body extracts were not affected by the protocol either (Figure 6). However, for the gut extracts, bead beating resulted in a 2-fold higher abundance of CEs (P = 0.033), and the DF step returned a higher abundance of CEs (2.2-fold, P = 0.016). The buffer choice influenced CE abundance in the gut extracts, with the SDS extraction buffer providing a 2-fold higher abundance of CEs as compared to the UTC buffer (P = 0.0495). P1 was the most effective protocol. The apparent abundance of the POs in the body extracts was affected by the inclusion of the DF step: NDF extracts returned ~32% higher abundance than the DF extracts (P = 0.027), however, no such effect was seen for the gut extracts. Finally, there was an effect of DF on the relative abundance of the lipases in the body extracts; the NDF extracts returned a 57% higher relative abundance compared to the DF extracts (P = 0.031). It is interesting to note that the relative abundances of the P450s in both tissues and the relative abundances of the POs and lipases in body tissue were reduced with the inclusion of the DF step. Only gut CEs were more visible with the addition of the DF step.

Metaproteome Analysis of the BSF Larval Gut. In total, 4964 unique peptides were detected within the aggregate BSF larval gut mass spectral data. Upon initial filtering, 54 peptides were removed, leaving 4910 peptides of which 39.6% (1943 peptides) were not taxonomically assignable, that is, the peptides sequences were highly conserved such that they could not be specifically taxonomically assigned. The remaining 60.4% proceeded to further taxonomic classification. At the level of "Organism," 705 peptides were specific to this level. A small proportion of the total assignable peptides (6.3%, 188 peptides) were assigned to the bacterial kingdom (Figure 7; Supporting Information File S2). Further inspection revealed that the assigned bacterial peptides were predominantly derived from the *Actinobacteria* (75 peptides), *Proteobacteria* (39 peptides), and *Firmicutes* (8 peptides) phyla. The Actinobacteria peptides had representation from the *Micrococcales* (27 peptides) and *Corynebacteriales* (11 peptides) genera. There was also representation from the *Bifidobateriales*, *Proprionibacteriales*, *Streptomyces*, and *Micromonosporales* genera. Most of the *Proteobacteria* assigned peptides were derived from the *Gammaproteobacteria* class (33 peptides). The majority (26) of these were assigned to *Enterobacterales* order; however, the peptides were highly conserved, so assignment to a specific genus within the *Enterobacteriaceae* family was not possible.

DISCUSSION

The biology and deep phenotypes of this recently "domesticated" species must be far better understood to ensure efficient uptake and use of BSF for such applications. We had initially set out to optimize the extraction of proteins from BSF larvae to obtain a baseline larval proteome for later comparison with future feeding and selection trails. However, given the rapid throughput of modern proteomic instrumentation, workflows, and data analyses, the question of the complementary of the proteomes obtained from the differing extraction protocols soon arose. We went on to test the hypothesis that the various protocols would provide a diversity of protocol-specific proteomes and that an aggregated NR set of proteins would provide a larger and more informative proteome.

Complementarity of Protocol-specific Proteins Sets to Generate the BSF Larval Body and Gut Proteomes. Due to lipids and non-protein components in animal tissues, a DF step is often included in the protein extraction process as excess lipid may interfere with chromatography and subsequently alter the proteome composition.[18,24] The inclusion of a DF step on larval body tissue substantially reduced the overall protein yield and the numbers of proteins and peptides identified. This is mostly due to the loss of proteins during the

https://doi.org/10.1021/acsomega.2c04462
ACS Omega 2023, 8, 7319−7330

DF and resolubilization steps.[19] When we investigated the influence of protocols on the relative abundances of targeted metabolic/detoxification enzyme classes, we found body P450s sensitive to mechanical disruption method, that is, liquid nitrogen was superior, as was solubilization with the UTC buffer. These results indicate that the use of several buffer compositions and complementary protocols can increase the proteome repertoire, but the optimization of targeted proteins of interest differs between sample types and extraction protocols.

Unlike the larval body, the benefits of combining protocol-specific gut proteomes were more readily apparent. Mechanical disruption method and the use of the DF step did not influence protein yield and numbers of proteins and peptides. Perhaps, this should not be surprising given the relatively homogenous structure and high cell density of gut tissue. However, while buffer choice did not affect total protein yields, extracts prepared with the UTC buffer returned significantly higher numbers of peptides (∼52%) and proteins (∼29%) than those extracts solubilized with the SDS buffer. There were large contributions of unique proteins from individual protocols (Figure 3C,D) reiterating the value of combining protocol-specific proteomes to build a comprehensive proteome database for gut tissue at least. When the gut protocol-specific proteomes were investigated for the presence of bacterial proteins, we found that bacterial proteins represented 6% or more of the detected proteins with DF combined with UTC solubilization protocols (P3 and P7), providing the most bacterial protein identifications (Figure 3E). Notably, the relative abundances of the gut P450s and CEs, as determined by MRM, were significantly influenced by mechanical disruption, DF, and buffer choice.

Unpacking the Larval Body and Gut Proteomes. In total, ∼73% of the larval body proteome was associated with binding functions, including transport of molecules of all classes within the cell, across cell membranes, and extracellularly (Figure 4A,C). Proteins associated with oxidation and reduction processes were the most abundant in the body tissue in the present study and in a previous study of three developmental stages of BSF,[14] reflecting the essential roles of redox chemistry as a foundation for biochemical reactions, such as glycolysis/gluconeogenesis metabolic pathways, during the pupae development. The gut proteome samples were enriched (GO terms) with a higher assignment of catalytic and hydrolysis activity (Figure 5A,C) compared to the body proteome (28%) reflecting the unique functions of the larval gut.

The hydrolase activity associated with the larval body and gut proteome was further investigated to identify its role in the various physiological processes (Figures 4B,D; 5B,D). We found two subclasses, acting on anhydrides and acting on peptide bonds, that are significantly dominant within hydrolase subclasses and play a role in solute transport, ATPases, and regulating peptidase and proteinase activities required for feed metabolism and tissue turnover and remodeling. The morphological and transcriptomic analysis of the BSF larvae midgut has shown the unique digestive and transformative capabilities that helps them to adapt to different food substrates.[25] Aligned with the findings from the present study, proteome analysis of BSF larval developmental stages revealed three physiological processes, including the insulin pathway for feed metabolism, fatty acid synthesis, and immune regulatory pathways.[9,10]

The gut metaproteomic analysis that was performed in this study also enabled some insight to the diversity of bacterial genera. *Actinobacteria*, and more specifically the *Actinomycetia* order, returned the largest number of peptides, and *Proteobacteria* was the second major contributor, with most peptides derived from the *Gammaproteobacteria* class. Surprisingly, very few peptides from *Bacteriodetes* and *Firmicutes* were detected, suggesting a low abundance of these bacterial communities in the larval gut. Microbiome studies of BSF larval midgut on standard or food waste diets have generally reported the converse; that is, the *Proteobacteria* and *Bacteriodetes* as dominant orders,[26] variable contributions from the *Firmicutes*,[27] and modest to minor contributions from *Actinobacteria* to the larval gut microbiome.[28] The BSF larval gut microbiome can be influenced by diet and larval age.[15,29] Akin to the present study, proteomics-based studies revealed the presence of defensin-like antimicrobial peptides[4] and phenoloxidases.[30] Our metaproteomic study results revealed Actinobacteria as the major order, which agrees with the findings from Klammsteiner and co-workers,[15,29] where the BSF larvae were raised on chicken feed. A future study should include various dietary regimens and larval and adult stages to further assess the gut microbiome diversity of BSF larvae, as their microbial presence controls their fitness and efficiency to upcycle waste material.[31]

CONCLUSIONS

In the present study, we embarked on the optimization of protein extraction from the BSF larval body and gut for analysis by LC-MS-based proteomics by comparing the extracts generated from protocols consisting of various combinations of mechanical disruption, use of a defatting step or not, and different solubilization reagents. Traditional measures, such as total protein yield and numbers of identified proteins and peptides, were an initial basis of assessment. However, we came to query our rationale on the basis that surely better coverage of the proteomes would be achieved by combining the plethora of gut or body proteomes generated by the suite of extraction protocols. The most informative measures were the numbers of unique proteins contributed by the protocol, the deeper level 4 GO terms (e.g., the hydrolase subclasses) and microbial protein identifications in the gut tissue. Overall, using complementary extraction protocols with discovery and targeted proteomics to establish the proteome and metaproteome would be useful for future research on BSF larvae.

ASSOCIATED CONTENT

Supporting Information

The Supporting Information is available free of charge at https://pubs.acs.org/doi/10.1021/acsomega.2c04462.

Materials and methods; detailed protocol for BSF larvae body and tissue processing; additional results on BSF larval proteome analysis; and number of peptide spectra detected (global 95% confidence and % of spectra match calculated for individual samples) following eight extraction protocols (P1−P8) from the body and gut of the black soldier fly (*H. illucens*) (PDF)

https://doi.org/10.1021/acsomega.2c04462
ACS Omega 2023, 8, 7319−7330

AUTHOR INFORMATION

Corresponding Authors

Utpal Bose − *CSIRO Agriculture and Food, St Lucia, Queensland 4067, Australia; Australian Research Council Centre of Excellence for Innovations in Peptide and Protein Science, School of Science, Edith Cowan University, Joondalup, Western Australia 6027, Australia; School of Pharmacy, The University of Queensland, Brisbane, Queensland 4067, Australia;* orcid.org/0000-0003-1156-6504; Email: utpal.bose@csiro.au

James A. Broadbent − *CSIRO Agriculture and Food, St Lucia, Queensland 4067, Australia;* orcid.org/0000-0002-0733-3639; Email: james.broadbent@csiro.au

Authors

Angela Juhasz − *Australian Research Council Centre of Excellence for Innovations in Peptide and Protein Science, School of Science, Edith Cowan University, Joondalup, Western Australia 6027, Australia;* orcid.org/0000-0002-4317-2027

Sally Stockwell − *CSIRO Agriculture and Food, St Lucia, Queensland 4067, Australia*

Sophia Escobar-Correas − *CSIRO Agriculture and Food, St Lucia, Queensland 4067, Australia; Australian Research Council Centre of Excellence for Innovations in Peptide and Protein Science, School of Science, Edith Cowan University, Joondalup, Western Australia 6027, Australia; CSIRO Agriculture and Food, Brisbane, Queensland 4001, Australia;* orcid.org/0000-0003-0712-691X

Anna Marcora − *School of Pharmacy, The University of Queensland, Brisbane, Queensland 4067, Australia;* orcid.org/0000-0001-6624-2553

Cate Paull − *School of Pharmacy, The University of Queensland, Brisbane, Queensland 4067, Australia*

Gene Wijffels − *CSIRO Agriculture and Food, St Lucia, Queensland 4067, Australia*

Complete contact information is available at: https://pubs.acs.org/10.1021/acsomega.2c04462

Notes

The authors declare no competing financial interest.

Raw and processed mass spectrometry have been submitted to the ProteomeXchange Consortium via PRIDE (project accession number: PXD037977). The username: reviewer_pxd037977@ebi.ac.uk and password: xId3kLNM.

ACKNOWLEDGMENTS

The authors would like to acknowledge the support from the interchange program and the Future Protein Mission from CSIRO. The authors would also like to acknowledge the anonymous reviewers for their constructive comments and suggestions during the revision process.

REFERENCES

(1) Henry, M.; Gasco, L.; Piccolo, G.; Fountoulaki, E. Review on the use of insects in the diet of farmed fish: past and future. *Anim. Feed Sci. Technol.* **2015**, *203*, 1−22.

(2) Li, Q.; Zheng, L.; Qiu, N.; Cai, H.; Tomberlin, J. K.; Yu, Z. Bioconversion of dairy manure by black soldier fly (Diptera: Stratiomyidae) for biodiesel and sugar production. *Waste Manag.* **2011**, *31*, 1316−1320.

(3) Choi, Y.-C.; Choi, J.-Y.; Kim, J.-G.; Kim, M.-S.; Kim, W.-T.; Park, K.-H.; Bae, S.-W.; Jeong, G.-S. Potential usage of food waste as a natural fertilizer after digestion by Hermetia illucens (Diptera: Stratiomyidae). *Int J Indust Entomol* **2009**, *19*, 171−174.

(4) Zhang, J.; Li, J.; Peng, Y.; Gao, X.; Song, Q.; Zhang, H.; Elhag, O.; Cai, M.; Zheng, L.; Yu, Z.; Zhang, J. Structural and functional characterizations and heterogenous expression of the antimicrobial peptides, Hidefensins, from black soldier fly, Hermetia illucens (L.). *Protein Expr. Purif.* **2022**, *192*, 106032.

(5) (a) Mouithys-Mickalad, A.; Schmitt, E.; Dalim, M.; Franck, T.; Tome, N. M.; van Spankeren, M.; Serteyn, D.; Paul, A. Black Soldier Fly (Hermetia Illucens) Larvae Protein Derivatives: Potential to Promote Animal Health. *Animals* **2020**, *10*, 941. (b) Zarantoniello, M.; Randazzo, B.; Truzzi, C.; Giorgini, E.; Marcellucci, C.; Vargas-Abúndez, J. A.; Zimbelli, A.; Annibaldi, A.; Parisi, G.; Tulli, F.; Riolo, P.; Olivotto, I. A six-months study on Black Soldier Fly (Hermetia illucens) based diets in zebrafish. *Sci. Rep.* **2019**, *9*, 8598.

(6) Barragan-Fonseca, K. B.; Dicke, M.; van Loon, J. J. Nutritional value of the black soldier fly (Hermetia illucens L.) and its suitability as animal feed—a review. *J. Insects Food Feed* **2017**, *3*, 105−120.

(7) Zhan, S.; Fang, G.; Cai, M.; Kou, Z.; Xu, J.; Cao, Y.; Bai, L.; Zhang, Y.; Jiang, Y.; Luo, X.; Xu, J.; Xu, X.; Zheng, L.; Yu, Z.; Yang, H.; Zhang, Z.; Wang, S.; Tomberlin, J. K.; Zhang, J.; Huang, Y. Genomic landscape and genetic manipulation of the black soldier fly Hermetia illucens, a natural waste recycler. *Cell Res.* **2020**, *30*, 50−60.

(8) Leni, G.; Prandi, B.; Varani, M.; Faccini, A.; Caligiani, A.; Sforza, S. Peptide fingerprinting of Hermetia illucens and Alphitobius diaperinus: Identification of insect species-specific marker peptides for authentication in food and feed. *Food Chem.* **2020**, *320*, 126681.

(9) Lu, L.; Wan, Q.; Xu, Y.; Shen, H.; Yang, M. Proteomic study reveals major pathways regulating the development of Black Soldier Fly. *J. Proteome Res.* **2021**, *20*, 2216−2223.

(10) Lin, Y.-B.; Rong, J.-J.; Wei, X.-F.; Sui, Z.-X.; Xiao, J.; Huang, D.-W. Proteomics and ultrastructural analysis of Hermetia illucens (Diptera: Stratiomyidae) larval peritrophic matrix. *Proteome Sci.* **2021**, *19*, 7.

(11) Varunjikar, M. S.; Belghit, I.; Gjerde, J.; Palmblad, M.; Oveland, E.; Rasinger, J. D. Shotgun proteomics approaches for authentication, biological analyses, and allergen detection in feed and food-grade insect species. *Food Control* **2022**, *137*, 108888.

(12) Belghit, I.; Lock, E.-J.; Fumière, O.; Lecrenier, M.-C.; Renard, P.; Dieu, M.; Berntssen, M. H.; Palmblad, M.; Rasinger, J. D. Species-specific discrimination of insect meals for aquafeeds by direct comparison of tandem mass spectra. *Animals* **2019**, *9*, 222.

(13) Tanga, C. M.; Waweru, J. W.; Tola, Y. H.; Onyoni, A. A.; Khamis, F. M.; Ekesi, S.; Paredes, J. C. Organic waste substrates induce important shifts in gut microbiota of Black Soldier Fly (Hermetia illucens L.): coexistence of conserved, variable, and potential pathogenic microbes. *Front. Microbiol.* **2021**, *12*, 635881.

(14) Callegari, M.; Jucker, C.; Fusi, M.; Leonardi, M. G.; Daffonchio, D.; Borin, S.; Savoldelli, S.; Crotti, E. Hydrolytic profile of the culturable gut bacterial community associated with Hermetia illucens. *Front. Microbiol.* **2020**, *11*, 1965.

(15) Klammsteiner, T.; Walter, A.; Bogataj, T.; Heussler, C. D.; Stres, B.; Steiner, F. M.; Schlick-Steiner, B. C.; Arthofer, W.; Insam, H. The core gut microbiome of black soldier fly (Hermetia illucens) larvae raised on low-bioburden diets. *Front. Microbiol.* **2020**, *11*, 993.

(16) Jing, T.-Z.; Qi, F.-H.; Wang, Z.-Y. Most dominant roles of insect gut bacteria: digestion, detoxification, or essential nutrient provision? *Microbiome* **2020**, *8*, 38.

(17) Bose, U.; Broadbent, J. A.; Juhász, A.; Karnaneedi, S.; Johnston, E. B.; Stockwell, S.; Byrne, K.; Limviphuvadh, V.; Maurer-Stroh, S.; Lopata, A. L.; Colgrave, M. L. Protein extraction protocols for optimal proteome measurement and arginine kinase quantitation from cricket Acheta domesticus for food safety assessment. *Food Chem.* **2021**, *348*, 129110.

(18) Bose, U.; Broadbent, J. A.; Juhász, A.; Karnaneedi, S.; Johnston, E. B.; Stockwell, S.; Byrne, K.; Limviphuvadh, V.; Maurer-Stroh, S.; Lopata, A. L.; Colgrave, M. L. Comparison of protein extraction protocols and allergen mapping from black soldier fly Hermetia illucens. *J. Proteonomics* **2022**, *269*, 104724.

(19) Bose, U.; Broadbent, J.; Byrne, K.; Hasan, S.; Howitt, C. A.; Colgrave, M. L. Optimisation of protein extraction for in-depth profiling of the cereal grain proteome. *J. Proteonomics* **2019**, *197*, 23−33.
(20) Bose, U.; Byrne, K.; Howitt, C.; Colgrave, M. L. Targeted proteomics to monitor the extraction efficiency and levels of barley α-amylase trypsin inhibitors that are implicated in non-coeliac gluten sensitivity. *J. Chromatogr. A* **2019**, *1600*, 55−64.
(21) Shilov, I. V.; Seymour, S. L.; Patel, A. A.; Loboda, A.; Tang, W. H.; Keating, S. P.; Hunter, C. L.; Nuwaysir, L. M.; Schaeffer, D. A. The Paragon Algorithm, a next generation search engine that uses sequence temperature values and feature probabilities to identify peptides from tandem mass spectra. *Mol. Cell. Proteomics* **2007**, *6*, 1638−1655.
(22) Khan, A.; Mathelier, A. Intervene: a tool for intersection and visualization of multiple gene or genomic region sets. *BMC Bioinf.* **2017**, *18*, 287.
(23) Gurdeep Singh, R.; Tanca, A.; Palomba, A.; Van der Jeugt, F.; Verschaffelt, P.; Uzzau, S.; Martens, L.; Dawyndt, P.; Mesuere, B. Unipept 4.0: functional analysis of metaproteome data. *J. Proteome Res.* **2018**, *18*, 606−615.
(24) Gravel, A.; Marciniak, A.; Couture, M.; Doyen, A. Effects of hexane on protein profile, solubility and foaming properties of defatted proteins extracted from Tenebrio molitor larvae. *Molecules* **2021**, *26*, 351.
(25) Bonelli, M.; Bruno, D.; Brilli, M.; Gianfranceschi, N.; Tian, L.; Tettamanti, G.; Caccia, S.; Casartelli, M. Black soldier fly larvae adapt to different food substrates through morphological and functional responses of the midgut. *Int. J. Mol. Sci.* **2020**, *21*, 4955.
(26) Zhineng, Y.; Ying, M.; Bingjie, T.; Rouxian, Z.; Qiang, Z. Intestinal microbiota and functional characteristics of black soldier fly larvae (Hermetia illucens). *Ann. Microbiol.* **2021**, *71*, 13.
(27) Tegtmeier, D.; Hurka, S.; Klüber, P.; Brinkrolf, K.; Heise, P.; Vilcinskas, A. Cottonseed press cake as a potential diet for industrially farmed black soldier fly larvae triggers adaptations of their bacterial and fungal gut microbiota. *Front. Microbiol.* **2021**, *12*, 634503.
(28) Bruno, D.; Bonelli, M.; Cadamuro, A. G.; Reguzzoni, M.; Grimaldi, A.; Casartelli, M.; Tettamanti, G. The digestive system of the adult Hermetia illucens (Diptera: Stratiomyidae): morphological features and functional properties. *Cell Tissue Res.* **2019**, *378*, 221−238.
(29) Klammsteiner, T.; Walter, A.; Bogataj, T.; Heussler, C. D.; Stres, B.; Steiner, F. M.; Schlick-Steiner, B. C.; Insam, H. Impact of processed food (canteen and oil wastes) on the development of black soldier fly (Hermetia illucens) Larvae and their gut microbiome functions. *Front. Microbiol.* **2021**, *12*, 20.
(30) Rabani, V.; Cheatsazan, H.; Davani, S. Proteomics and lipidomics of black soldier fly (Diptera: Stratiomyidae) and blow fly (Diptera: Calliphoridae) larvae. *J. Insect Sci.* **2019**, *19*, 29.
(31) Tettamanti, G.; Van Campenhout, L.; Casartelli, M. A hungry need for knowledge on the black soldier fly digestive system. *J. Insects Food Feed* **2022**, *8*, 217−222.

NOTE ADDED AFTER ASAP PUBLICATION

This paper originally published ASAP on February 20, 2023. A misspelling in the title was corrected, and a new version reposted on February 28, 2023.

https://doi.org/10.1021/acsomega.2c04462
ACS Omega 2023, 8, 7319−7330